

DEVELOPMENT OF HYDROGEN LOADING SYSTEM AND CHARACTERIZATION OF TRITIATED METALLIC FILMS FOR BETAVOLTAIC BATTERIES

Thomas E. Adams

School of Nuclear Engineering
Purdue University
West Lafayette, IN 47905, USA
Email: adams30@purdue.edu

Shripad T. Revankar

School of Nuclear Engineering
Purdue University
West Lafayette, IN 47905, USA

ABSTRACT

Currently, no portable power source extends beyond 10 years in extreme temperature environments, e.g. -40°C to 80°C. Conventional electrochemical batteries do not perform well at extreme temperatures and rarely operate longer than 5 years; thermally induced performance degradation is common. However, commercial betavoltaic batteries can operate in excess of 10 years over extreme temperatures. Potential applications for low-power betavoltaic sources may be found in distributed power systems, sensors, remote power, and bio-medical devices & implants. Betavoltaic technology is rapidly maturing, giving rise to numerous areas of research and development, e.g. beta source and semiconductor efficiency. This study presents an update on some current aspects of betavoltaics, challenges existing within the technology, and research and development currently being conducted. The substrate material that serves as the sync or storage medium for the radioisotope source has become a significant challenge due to issues associated with loading techniques, thin-film properties, beta-particle interaction, and defect damage. Recent betavoltaic designs invoking tritium stored as tritides in titanium and scandium demonstrated a number of practical difficulties yielding to material damage and inconsistent tritium concentrations. Various material modifications and hydrogen loading techniques are being evaluated to proof new methods, materials and designs that result in less expensive tritiated foils with consistent concentrations. Modeling experiments are being conducted to verify and validate the loading and storage mechanism of tritium in the metal hydrides.

INTRODUCTION

Radiation interaction with materials can have beneficial uses, such as in betavoltaic cells, a type of radioisotope power source where the kinetic energy associated with beta (β^-) decay is converted into electricity. Though not a new concept, research and development has been minimal for many years due to limited low-power applications, rapid semi-conductor degradation, limited availability and high cost of suitable radioisotopes, and public perception. Novel and compelling need-based applications are emerging in the military, intelligence, commercial, and medical markets that can utilize the diminutive energy produced from such cells. Present-day micro-electromechanical systems and electronic devices make betavoltaics an attractive alternative to electrochemical batteries enabling applications to perform for much longer periods in extreme temperatures. Unlike conventional electrochemical batteries, commercially available betavoltaics can operate in excess of 10 years over temperatures ranging from -55°C to 150°C [1]. Because the technology is far from mature, many challenges and issues remain to be solved to improve efficiency and energy density, and reduce cost, which will be discussed in the background section of this paper.

In tritium based designs, the substrate material that serves as the sync or storage medium for the tritium has become a significant challenge. Tritium can be efficiently stored as a solid in metal rather than as a compressed gas. Palladium (Pd) can store up to 900 times its volume of hydrogen at room temperature leading to an H:Pd ratio of 0.6 [2, 3]. Scandium (Sc) and titanium (Ti) can store larger amounts of hydrogen by forming hydrides, ScH₂ and TiH₂. Recent beta source designs

invoking tritium stored as tritides demonstrated a number of practical difficulties with loading techniques and substrate damage. Air and moisture contaminate the surface which increases the activation energy necessary for diffusion. Substrates around 500 nm thick are necessary to efficiently fuel betavoltaics due to shielding from the metallic substrate. The current method in producing tritiated films is rather expensive, time consuming, not consistent, and not well understood.

To better understand the hydrogen (Protium, Deuterium and Tritium) absorption process in thin films, a hydrogen loading system capable of pressures and temperatures of 1000 psi and 500°C, respectively, was designed and built. Initial experiments are being conducted at pressures less than 1 bar to simulate the present loading system being developed by industry. A four-wire probe was incorporated to perform in situ resistivity measurements to understand the thermodynamics during hydrogen loading and unloading. Resistivity is a measurement that can provide useful information about the film as it hydrides. such as interface contact, number of conduction electrons, and surface contamination. Absorbed hydrogen is quantified by accurate temperature and pressure measurements.

Various types of thin film substrates are being investigated to determine if combinations of metal storage materials with a catalyst lower the energy needed for hydrogen loading and hydrogen retention. The loading process of Pd films is not difficult due to a cleaner surface and a catalytic effect. Recently developed graphene films may provide a better substrate at a much lower cost. Graphene (~2.0 g/cm³) has a lower density than Sc (3.0g/cm³) and Ti (4.5 g/cm³), but has a comparable hydrogen density when fully loaded: graphene (0.12 kg/L), Sc (0.13 kg/L) and Ti (0.18 kg/L) [4]. The beta flux and energy distribution at the surface of these fully loaded tritiated films are being simulated using MC-SET (Monte Carlo Simulation of Electron Trajectories in solids) [5].

Little performance data exists on current betavoltaic technology. Furthermore, temperature behavior and aging phenomena are not known. Two betavoltaic cells made by City Labs were obtained from Air Force Research Laboratories (AFRL) and are being evaluated under temperature. The results will provide a benchmark for the design, an understanding on how they operate, and a basis to determine if a correlation exists with solar activity [6].

BACKGROUND

Radioisotopes are encountered daily and are used safely in many applications with some shown in Figure 1, such as for households, hospitals, retail stores and aircraft. Smoke detectors rely on americium-241 (²⁴¹Am) for sensing smoke. Hospitals use x-ray machines, chemotherapy, and tracers daily in many of the protocols. Tritium (³H) is currently used to provide illumination, such as in exit signs, gun sights and wrist watches. Promethium-147 (¹⁴⁷Pm) has been used to illuminate gauges for aircraft. Bananas naturally contain trace amounts of

potassium-40 (⁴⁰K). Studies have also shown that an office building receives a larger dose of radiation from the Sun and space than inside a nuclear power plant. The stringent requirements of the Nuclear Regulatory committee (NRC) often delay development until a general license or a sealed source and device permit is granted, which can take a year or more because of testing and the approval process.



Figure 1. Examples of use of radioisotopes

Betavoltaic Electrical Conversion

A direct conversion betavoltaic is comprised of two components, the p-n junction and the beta source. Electricity is produced similar to a photovoltaic using the kinetic energy of the beta particles. The basic concept of operation is shown in Figure 2. Beta particles enter the p-n junction and collide with atoms creating electron-hole pairs (EHPs) as they slow down. A 5 keV particle creates over 1000 EHPs, and deposits some energy into the lattice. In the depletion region, holes are accelerated to the p-side collector and the electrons are accelerated to the n-side collector. EHPs created outside the depletion layer quickly recombine and provide a net current of zero. With a load connected, the electrons travel from the n-side, through the load and back to the p-side. Because EHP exhibit relatively short lives, the voltage developed is a function of the semiconductor material and energy of the beta particle.

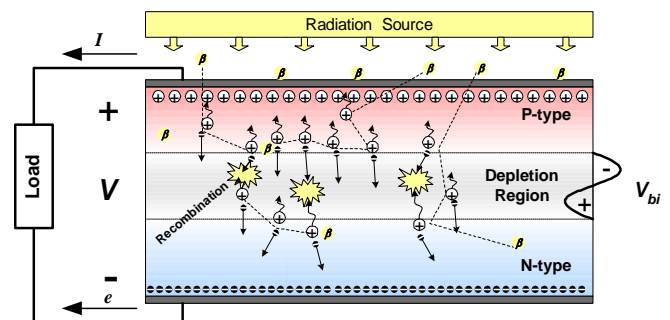


Figure 2. Voltaic Operation; conversion of radiation into electricity.

The electrical output of a betavoltaic resembles that of a diode as shown in the normalized plot in Figure 3. The peak power occurs about 0.8 times open-circuit voltage (V_{oc}). Two modes of operation exist: before the peak power point is

constant current mode and after the peak power point is constant voltage mode.

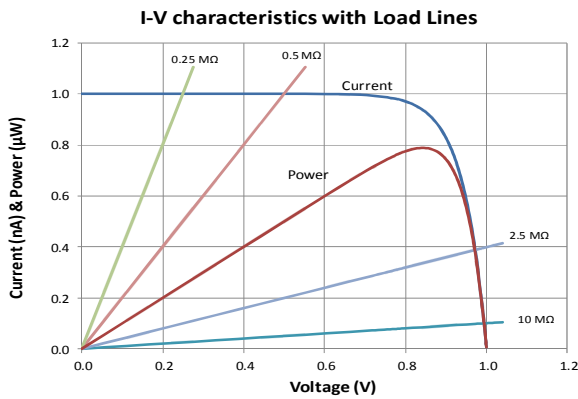


Figure 3. Betavoltaic power characteristics.

Hybrid designs consisting of a betavoltaic and rechargeable battery or capacitor are being explored to provide both latent and burst power. The basic schematic of a hybrid design is shown in Figure 4. The betavoltaic will trickle charge the battery or capacitor. Because betavoltaics are high impedance devices, additional circuitry may be needed to match the lower impedance of the battery. With capacitors, the effective series resistance must be considered.

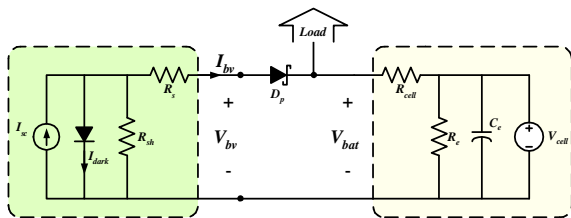


Figure 4. Hybrid betavoltaic and battery.

History of Betavoltaics

The first betavoltaic battery was developed in 1953 at RCA by Rappaport. The device yielded an efficiency of only 0.2% and degraded rapidly due to radiation damage from strontium-90 (^{90}Sr) [7]. Several others continued research using promethium-147 (^{147}Pm) but were only able to achieve <1% efficiency [8, 9]. The most promising effort in betavoltaics occurred in *ca.* 1974 through research led by Olsen at the Donald W. Douglas Laboratories [10]. The Betacel battery, shown in Figure 5, exhibited 400 μW and a 4% efficiency using ^{147}Pm and silicon p-n junctions. The Betacel was used in pacemakers that were implanted in over 285 patients, 60 inside the United States. German and U.S. medical institutions were seriously considering the Betacel for wider use. The United States Atomic Energy Commission (USAEC) had authorized the licensing of 50 Betacel pacemakers per month [11]. However, strides in lithium battery development entered onto

the scene and were subsequently selected for pacemakers instead [10]. In the last 10 years, designs using tritium and amorphous silicon, and krypton-85 (^{85}Kr) and silicon carbide (SiC), and nickel-63 (^{63}Ni) and SiC, exhibited high degradation rates [12-14]. Others are researching indirect methods of energy conversion to avoid semiconductor degradation issues.

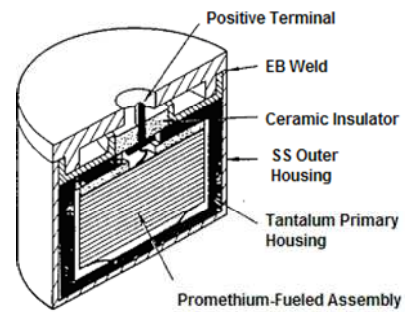


Figure 5. 400 μW Betacel battery [10].

Recent research and development has concentrated on designs using tritium for its low radiation energy, ease in shielding and availability. Tritium is used in many products for illumination, such as exit signs, gun sights, and watches. A general license is required from the U.S. Nuclear Regulatory Commission (NRC) before the device can be purchased by anyone. City Labs, Inc. currently produces a tritium betavoltaic shown in Figure 6 that exhibits the highest an overall efficiency of 7.5%, and has been granted the first general license for betavoltaics by the NRC.



Figure 6. NanoTritium™ betavoltaics.

Challenges in Betavoltaic Technology

Challenge-goal based objectives have been established by the Defense Advanced Research Projects Agency [15] to pursue for developing futuristic betavoltaic cells: (1) 35 mW of continuous power output, (2) size 1 cm^3 , (3) <1% self-induced radiological degradation per year in power output, and (4) <500 mrems/year radiation leakage at 30 cm. To obtain the power in a one cm^3 package, the overall efficiency must increase dramatically beyond the 10 percent claimed maximum.

The overall efficiency is controlled by the beta source, electron-hole production and semiconductor substrate following Eqn. (1).

$$\eta_{overall} = \eta_{\beta} \eta_{conv} \eta_{sub} \quad (1)$$

The beta emission efficiency, η_{β} , is limited by self-shielding of the beta source, isotropic beta emission and reflections. The conversion efficiency, η_{conv} , includes the EHP generation rate and recombination rate. The substrate conversion efficiency, η_{sub} , is controlled by the geometry, doping and quality of semiconductor.

Beta energy spectrum

Beta decay does not occur at specific discrete energies; rather, the emitted electrons form a continuous energy spectrum which is different for each isotope. Figure 4 shows a generic beta energy spectrum. The average energy is typically one-third the maximum energy. Factors such as self-shielding and low enrichment reduce the quantity of betas that finally reach the betavoltaic converter device. The extent of self-shielding increases with isotope layer thickness and density. Another important factor is the penetration depth of the beta particle in material. The range is a function of the material's density and can be estimated using the relationship of Eqn. (1) for electron energy less than 2.5 MeV [16].

$$R_{max} * \rho = 0.412 E_{max}^{(1.265 - 0.0954 \ln E_{max})} \quad [g \cdot cm^2] \quad (1)$$

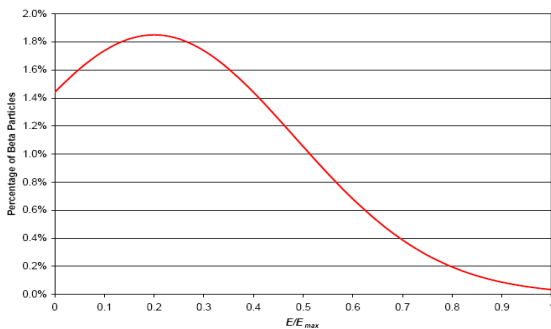


Figure 7. Normalized Beta Energy Spectrum

P-N junction

In choosing the base material for the p-n junction, the material density, band gap energy, and resistivity must be considered. Table 1 shows these characteristics for common semiconductors. High bandgap materials exhibit high open-circuit voltages and low reverse (dark) currents. However, the higher resistivity values indicate a high defect density which reduces the conversion efficiency. The surface and bulk resistivity of a semiconductor are a function of the number of defects (traps) and impurities [17]. A layer of intrinsic or

undoped semiconductor substrate can be left in-between the p-side and n-side to widen the depletion layer.

Table 1. Characteristics of common semiconductor materials at room temperature [18].

Property	Si	GaAs	4H SiC	GaN	AlN	Diamond
Density (g/cm ³)	2.33	5.40	3.21	6.10	3.26	3.52
Bandgap (eV)	1.1	1.43	3.26	3.45	6.2	5.45
Resistivity (Ω-cm)	1000	< 10 ⁸	> 10 ¹²	> 10 ¹⁰	> 10 ¹³	> 10 ¹³

Beta emitting source

When selecting a beta emitting isotope, the maximum beta energy and decay half-life are the most important criteria. The beta energy from ⁹⁰Sr and ⁸⁵Kr exceeds the minimum dislocation energy of 300 keV which results in semiconductor damage and bremsstrahlung [19]. The 25-day half-life of phosphorus-33 is too short for a long operating life. Therefore, of the three potential isotopes in Table 2, tritium is the most attractive. Tritium is readily available from Ontario Power in Canada and is least expensive at \$3.50/Ci. Russia is the only provider of ¹⁴⁷Pm and ⁶³Ni, which are costly at >\$1000/Ci [20] and \$4000/Ci [1], respectively. Reprocessing in the U.S. could help alleviate these obstacles making them attractive again for radioisotope power.

Table 2. Potential radioisotopes.

Isotope	T _{1/2} (yr)	E _{AVG} (keV)	E _{max} (keV)	Ci/g	W/g	Cost/Ci
Tritium	12.33	5.7	18.5	9,664	0.33	\$3.5
Ni-63	100.1	17.1	67	59	0.006	\$4,000
Pm-147	2.6	65	220	600	0.22	\$1,000

Tritium loading process

The tritium loading process is the major challenge for direct conversion betavoltaics; it is expensive, time consuming, and lacks control which results in inconsistent tritium concentrations and damage to films. The absorbing metal is typically deposited on stainless steel foils or silicon substrates. Tritium is currently loaded into thin films at Kinetics in Canada using a sealed system designed to capture unused tritium. The samples can be heated up to 500°C while the tritium pressure ranges from 1 bar up to 100 bar using a pump. A newer system is being built in Canada with better temperature control and tritium purity, but the pressure is limited to 1 bar. Therefore, the substrates must be heated to temperatures in excess of 400°C to initiate diffusion, and in many cases, the metallic film often becomes damaged due to tensile and compressive stresses develop at the thin-film/substrate interface due to tritium absorption and mismatches in thermal expansion. Such stresses can lead to delamination and buckling, similar to the growth of titanium oxide as shown in Figure 8 [21].

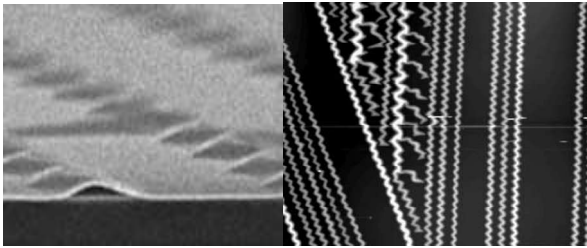


Figure 8. Delamination and buckling of TiO₂.

Minimal research

A literature survey was conducted using the Compendex Database accessed through the Purdue University's library portal in June 2013. Variations of betavoltaic were used as the search keyword. The results exhibited some interesting data on when articles were published and who published them as shown in Figure 9. Prior to 1976, only 12 articles were published. Since 1976, 138 journal articles were published, and of those, 104 or 75% were published in the last six years. Over 90% of the articles were published in the U.S. through 2007. Since then, the number of publications on betavoltaics by U.S. institutions dropped below 20%, while the number of publications for China increased to over 75%. Canada and Norway have been conducting some research and research is emerging in Korea, Italy, Australia and Iran.

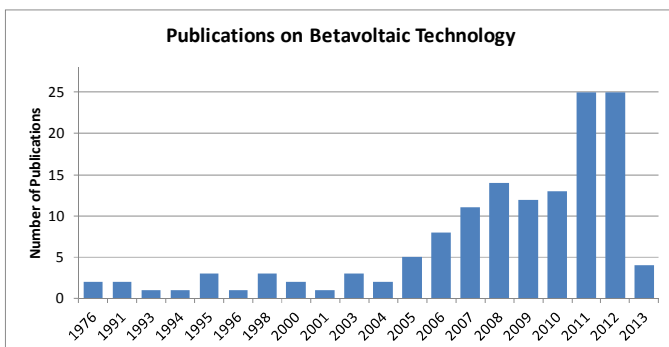


Figure 9. Publications by year since 1976 on Betavoltaic Technology based on Compendex Database generated on June 7, 2013

HYDROGEN LOADING SYSTEM

A system was needed that could accurately monitor the hydrogen absorption process into metallic films, such as temperature, pressure and resistivity. For a starting point, the system at Greenway Energy located in the Hydrogen Research laboratory at Savannah River National Lab (SRNL) was used to develop the following preliminary specifications:

- 1) Reactor that can hold many samples and withstand high temperatures and pressures of 500°C and 1000 psi.

- 2) Small control volume to provide better resolution for pressure measurements.
- 3) Wire feed-throughs for electrical measurements.
- 4) Accurate temperature, pressure, voltage and current measurements and control.

From here, the design was an iterative process by building system with available materials and components, evaluation and testing, and replacing with specific components. Parts and components designed for high pressure systems with extremely low leak rates are expensive. Care was taken in researching components and materials to ensure they satisfy physical and system requirements. Accurate volume calculations are necessary, especially at high pressures, in order to have the differential pressure transducer operating within its working range. Experiments consist of parametric studies by varying pressure and temperature, and studies based on phase diagrams.

System Design

The schematic of the hydrogen loading system (HLS) is shown in Figure 11 and contains 12 valves. The volume that is measured in experiments is referred as the Control Volume which consists of volumes 3 and 4. The Reference Volume consists of volume 5 and is used to provide a constant reference pressure on the high side of the differential pressure transducer (DPT). The calibrated 25 cc reservoirs are used to measure the other volumes by successively open valves one at a time. The volume between gas valves, vacuum valve and control volume is referred as volume 2 and can be used to adjust pressure. Volumes A and S and small volumes for fine pressure adjustments.

A 25 cubic centimeter (cc) reactor, shown in Figure 10, was designed collaboratively with Parr instruments (Moline, IL) to hold gasses, especially hydrogen, and certified up to 1000 psi at 500°C. The reactor in was designed. The reactor is made of 316 stainless steel and interior is 1" diameter by 2" high leading to a free volume of 25 cm³ (or cc).

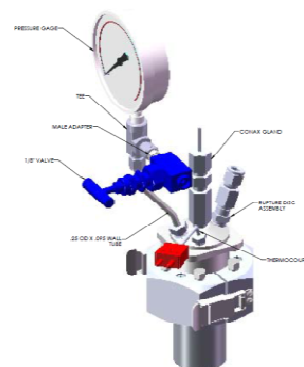


Figure 10. Parr Reactor Vessel

The reactor is heated by a ceramic Watlow heater controlled using an internal thermocouple. The top is removable and held onto the reactor with six bolts that are tightened to 25 inch-pounds using a torque wrench. The top has four ports: pressure relief valve, Conax four-wire gland, thermocouple and gas. Thermocouple probe enters vessel via a 1/8" Swagelok NPT fitting and Conax multiple element sealing flange is mounted to a standard 1/4" NPT located on the top. A safety relief valve rated at 1000 psi is for safety to prevent over-pressure conditions.

During experiments, the free volume is minimized to enhance the pressure difference measured by the DPT; this volume is measured with helium prior to hydrogen loading. Stainless steel slugs, type 316, of various thickness ranging from 0.1 inch to 1 inch were made to reduce the free volume of the reactor. The diameter of the slugs was 0.005" smaller than the reactor opening to prevent binding when the reactor is heated. The amount of hydrogen absorbed is determined by the difference in pressure before and after loading. For pressures below 5 bar, Eqn. (2) can be used with less than 1% error which is based on the ideal gas law where pressure P is in Pascal, volume V is in m^3 , the gas constant R is 8.314 J/mol/K, and temperature T is in K. At higher pressures, van der Waals equation of state in Eqn. 3 must be used instead of the ideal gas law to account for the molecular sizes and interaction forces [22]. Coefficient a (2.45×10^{-2} for H) accounts for molecular forces and coefficient b (26.61×10^{-6} for H) accounts for the molecular size.

$$\Delta P = \Delta n \frac{RT}{V} \quad (2)$$

$$\left[P + a \left(\frac{n}{V} \right)^2 \right] \left(\frac{V}{n} - b \right) = RT \quad (3)$$

At low pressures, the pressure difference ΔP is inversely proportional to volume and is proportional to temperature and the amount of moles absorbed, Δn . Therefore, pressure differential will always be the same regardless of the gas pressure.

Swagelok tubing, fitting and diaphragm valves are used to maintain and control a leak rate less than 10^{-7} cc/s. Two thermocouples, T_1 and T_2 , are fastened on the tubing from the Parr reactor to obtain the temperature gradient to calculate precise molar concentrations. Two pressure transducers, 100 bar and 3.5 bar, are used to monitor system pressure while. A Honeywell Smart 3000 differential pressure transducer (DPT) with a range of 1mbar to 1 bar is used to measure the change in pressure due to hydrogen absorption. As a safety precaution to noise from instrumentation, all components of the system are grounded to Earth.

The USB-2408 data acquisition device has 16 analog inputs, eight digital inputs/outputs (I/O) and two counters. Maximum sampling rate is 1000 readings per second. The channels can be configured for 16 single ended inputs or eight differential inputs. In the system, it is configured for eight differential inputs. Each channel has 24-bit resolution with $40 \mu V$ accuracy. Channels can be set to measure volts or thermocouples. The unit contains a built in reference thermocouple for temperature measurements.

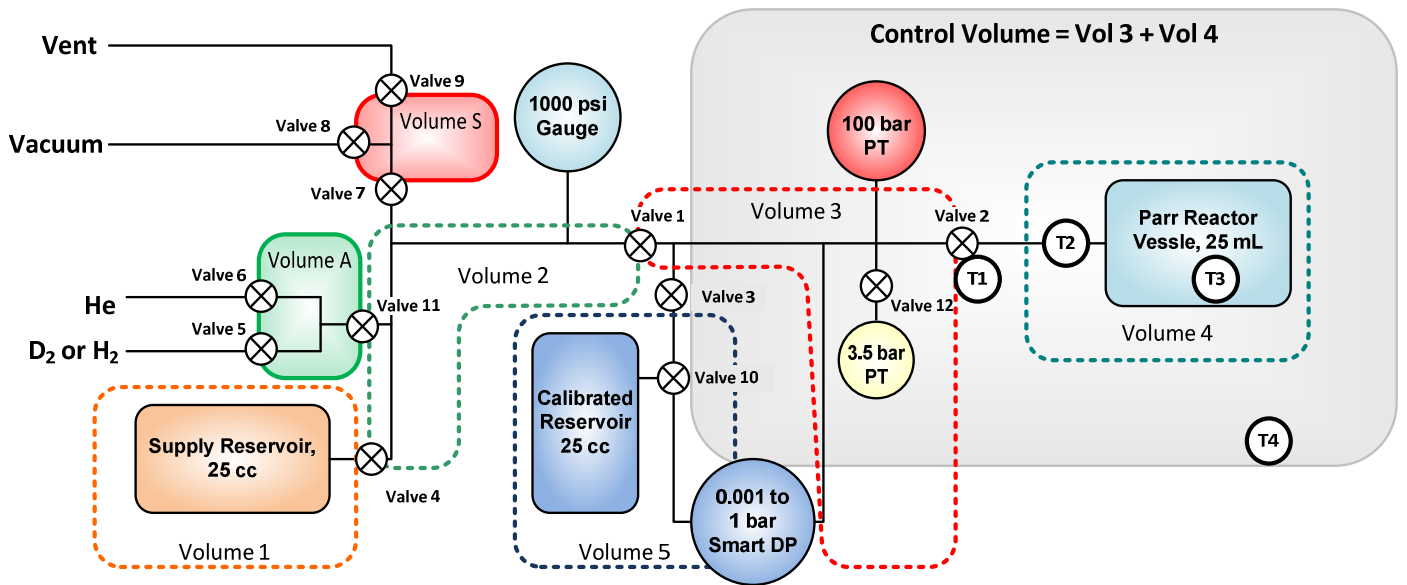


Figure 11. Hydrogen Loading System Schematic

A typical hydrogen loading experiment consists of sample setup, test setup, test and data analysis. Samples, spacers and resistivity probe will be placed in reactor and sealed. The reactor is heated to test temperature. Signal from pressure transducers and thermocouples are calibrated. After pulling a vacuum, the calibrated 25 cc reservoir, is filled with helium to a pressure of 3.5 to 20 bar, is used as a reference to calculate the volumes between valves. The valves of the system are opened one at a time to measure volumes by pressure drop and then checked for leaks. A simulation is done with helium to obtain free volume of reactor and initial pressure settings with the Parr valve. Two ~1 cc volumes are used for fine pressure adjustments. Finer adjustments are made with partially opened valves. Once correct pressure is obtained, helium is locked in volume 5 for DPT reference. When Parr valve is opened, the pressure should decrease to the same value as the reference, 0 bar or slightly above. Once correct pressure is obtained, helium is locked in volume 5 for DPT reference. The system is evacuated, except for the reference leg of the control volume. Now, the system is filled with hydrogen and allowed to equalize. Before opening Parr valve, the data acquisition system is started to capture initial measurements of temperature, pressure and resistance. When the DPT pressure profile stabilizes flattens, the absorption process is done, and the system returned to room temperature.

An example of the loading process is shown in Figure 12, where the system is pressurized with hydrogen first, and then the reactor is heated. The hydrogen activation in the films begins at a temperature of 320°C. The loading system is currently being validated by a similar system used at SRNL.

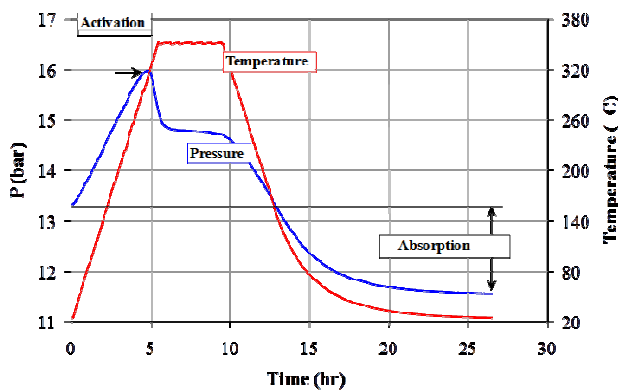


Figure 12. Typical loading profile

Resistivity Measurements

A four-wire Conax gland was added to the Parr reactor for *in situ* resistivity (ρ) measurements. The four-point probe method is used to make resistivity measurements of the film during hydrogen loading. The method has been used to characterize the behavior of the film during hydrogen

absorption and desorption [23, 24]. Each contact is separated by same 1.5 mm in a line. It is important to locate the probe in the center of the sample and that the same amount of contact force is made for each measurement. Measurements will be taken on the topmost thin-film sample by a Keithley dual channel source measurement unit (SMU) 2602B. Current is sourced through the outer contacts; the voltage drop is measured by the inner contacts.

BETA FLUX MODEL

Tritiated films need to be certain thickness to efficiently utilize tritium and optimize beta flux emitting from the surface which is a function of the material's density and tritium stoichiometry. Palladium can store hydrogen up to an atomic ratio of 1:1, but its high density of 12.03 g/cm³ shield much of the beta particles. Scandium has a density four times lower and can store an atomic ratio of 1:2. The ability to predict the beta particle flux and its energy distribution from the surface of a metal tritide is important in designing a film. A model has been developed using a software tool called MC-SET [5], and calculations. Simulations have been run on Pd and Ti to determine surface flux with its energy and angular distributions. Other potential storage materials are being simulated. Mathematical models will use the results to calculate flux and energy distribution by considering isotropic emission, emission energy, exit angle and material properties. Beta particles are emitted isotropically in a range of energy where the average energy is 30 percent of the maximum energy. The normalized energy spectrum of tritium is shown in Figure 13 with energy separated into 1 keV intervals. The beta energy decay probability was calculated using the beta energy distribution function given by Bower [20].

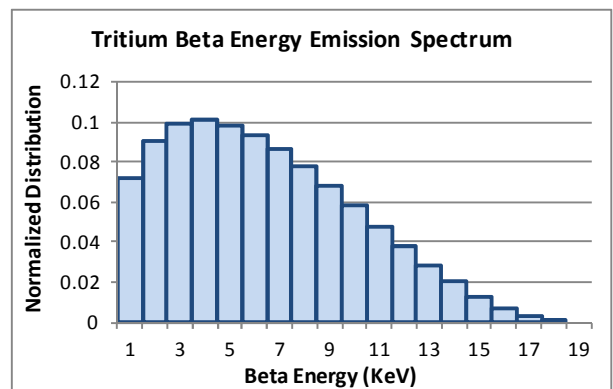


Figure 13. Relative decay probability of tritium.

Simulations were run on a Ti slab 2 μ m thick and on a Pd slab 1 μ m thick. The beam incidence point was normal to the surface and started at the bottom of the slab and moved up by 50 nm increments. At each incidence point, 18 simulations were run with 5000 electrons from 1 keV to 18 keV in increments of 1 keV [25]. The simulation results were

weighted with the energy distribution probability to produce a beta flux profile versus thickness. In Figure 14, the beta flux in Pd does not change beyond a thickness of 500 nm. For Ti, the beta flux does not change beyond a thickness of 1200 nm as shown in Figure 15. The percentage of beta particles emitted versus those that reach the surface decreases as the film gets thicker. The most efficient use of beta energy occurs in Ti films 300 nm thick, the point where the surface beta strength and percentage that reach the surface intersect, which corresponds closely with results published by Bower [20].

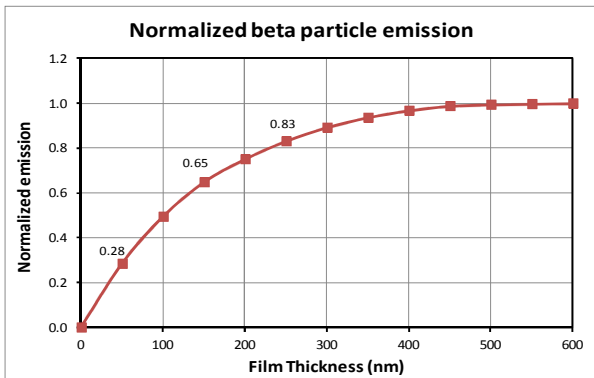


Figure 14. Tritium beta flux in Pd.

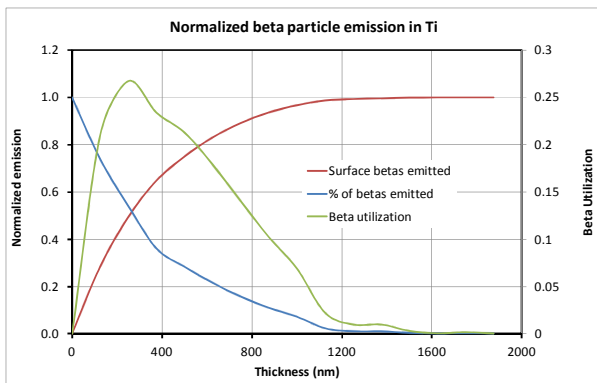


Figure 15. Tritium efficiency and utilization in Ti.

BETAVOLTAIC ELECTRICAL CHARACTERIZATION

Little performance data exists on current betavoltaic technology. Furthermore, temperature behavior and aging phenomena are not known. In the evaluation, I-V characteristics of each betavoltaic will be measured daily under temperature conditioning for several months. The setup consists of a temperature chamber, source measurement unit and a PC with data acquisition software. Monitor cables are 24 gauge twisted pair shielded to remove noise.

Temperature chamber is a Test Equity Model 107 which is programmable to operate from 132°C down to -40°C and does not require liquid nitrogen for cooling. Betavoltaics are tested inside the chamber. A chamber was programmed to the profile shown in where the temperature is cycled daily between 80°C, 25°C and -30°C. A thermocouple will monitor the temperature and store the readings in a separate standalone data logger installed on the PC. Ramp time between temperatures is one hour.

After several months of testing, the power profile at each temperature should follow the power curve similar to the decay rate calculated by Eqn. (4) where P_0 is the initial power, t is time in years, and half-life $T_{1/2}$ is the decay rate in years. With a tritium half-life of 12.3 years, the power will decrease by 2.78% after six months and 5.48% after one year. Therefore, accurate measurements are necessary and must be done the same way every time.

$$P(t) = P_0 e^{-\lambda t} = P_0 e^{-0.693 \times t / T_{1/2}} \quad (4)$$

Methods of measuring I-V curves on betavoltaics are not well defined. The impedance of betavoltaics are in the Megohm, thus four-wire measurements are not needed. Longer integration times in the seconds are required to obtain repeatable results. A capacitive term inside the betavoltaic does not allow voltage to change quickly. In the TSP control panel, the minimum and maximum source values are entered. Since the betavoltaic is supplying current, the source current is negative; a mistake in using positive current will damage the p-n junction [8].

Before applying an I-V sweep, the short circuit current and open circuit voltage are determined, and are used to input the range in the TSP software. Measurements have been conducted using 20 steps from 0 A to short-circuit current at a sampling rate of 5 seconds per reading. Voltage sourcing did not produce repeatable results. City Labs uses a Keithley 2400 SMU and takes an average of 10 measurements per step while sourcing voltage. A software program to conduct the measurements is being done externally. The method used in this evaluation will be replicated on the 2602B to make data compatible.

The most important characteristics used to gauge betavoltaic performance are open circuit voltage (V_{oc}), short circuit current (I_{sc}), maximum power and fill factor (FF), which is given in Equ. (5) as the ratio of maximum power (P_{max}) and the product of V_{oc} and I_{sc} . The higher the fill factor, the better the performance.

$$FF = \frac{P_{max}}{V_{oc} I_{sc}} \quad (5)$$

At room temperature, the initial open circuit test was conducted manually using the front panel of the SMU by setting source current to zero. Cell 1 exhibited 0.72 V and had proper polarity with respect to the betavoltaic specification. Cell 2 exhibited ~1.6 V but the polarity was reversed. The short circuit current was also measured using the front panel by setting the source voltage to zero.

I-V curves were taken at room temperature and at 80°C by varying integration time, source and steps. Measurements were done with sourced current (negative) and sourced voltage. Strange readings were obtained when voltage was sourced on Cell 1. The data from the measurements is summarized in Table 3.

Table 3. I-V data summary for Cell 1 and Cell 2

Test	T (°C)	V _{oc} (V)	I _{sc} (nA)	P _{max} (nW)	FF
Cell 1, 10-15-2013	25	0.72	73.00	36.23	0.690
Cell 1, 10-27-2013	25	0.72	73.03	31.85	0.603
Cell 1, 10-3-2013	80	0.65	52.92	19.58	0.572
Cell 1, 10-18-2013	80	0.54	45.03	6.43	0.266
Cell 2, 10-3-2013	25	1.65	60.31	77.49	0.779
Cell 2, 10-15-2013	25	1.58	60.69	79.09	0.822
Cell 2, 10-27-2013	25	1.60	60.00	61.62	0.644

The I-V curves for Cell 1 were acquired at room temperature and 80°C by sourcing current and measuring voltage. The reason for bad current measurements when sourcing voltage on Cell 1 is being investigated. However, good readings were acquired on Cell 2 with the voltage as the source. According to City Labs, the voltage is the proper source.

Results from Cell 1 at 25°C are plotted in Figure 16. The I-V curves are similar with an open circuit voltage of 0.72V and short circuit current of 73.0nA. Maximum power and fill factor deviated moderately by 3.5nW and 0.087 or 8.7%. This difference is too large for room temperature variations. The current should be more constant at low voltages up to about 0.6V.

Plots of the first two I-V tests run on Cell 2 are shown in Figure 17. Both tests were done 25°C by stepping the source voltage down from open circuit voltage to 0V; the Keithley only went down to 0.1 V instead of 0V, hence the reason for the gap near the vertical axis. The measured parameters were extremely close within 5% of each other. The current is 20% less than the single cell of Cell 1, but it is much flatter as should be expected. The voltage was about 15% higher. Since both cells are made from the same materials, the currents should be the same and the voltage of Cell 2 should be twice the voltage of Cell 1. The power values and fill factors were also higher by about 20%.

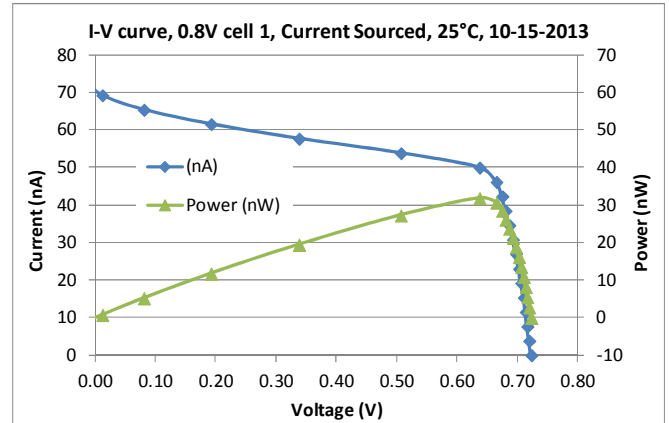


Figure 16. I-V curve for betavoltaic 0.8V cell #1 at 25°C; Current source, data recorded by Keithley 2602B SMU on 10-15-2013

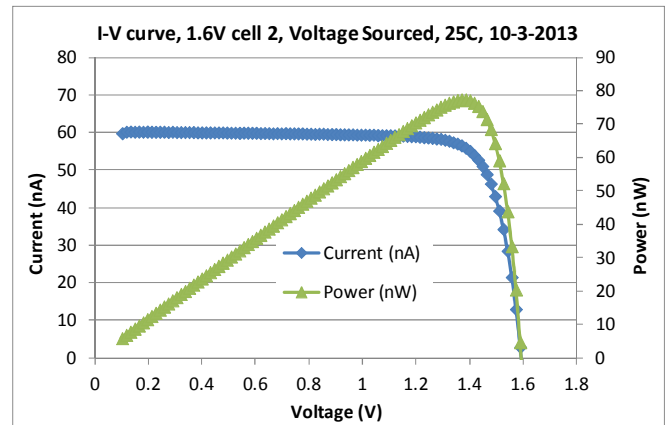


Figure 17. I-V curve for betavoltaic 1.6V cell #2 at 25°C; data recorded by Keithley 2602B SMU on 10-3-2013

CONCLUSION

Betavoltaic power sources are a safe enabling technology for military and commercial applications; very long operating life under harsh environmental conditions. The technology is far from maturity with much room for improvement. Many technical and ideas exist, but the level of research and support remains low. Understanding the film behavior during tritium loading process will lead to optimal and consistent tritium loadings that will lead to higher power, lower cost devices. The developed loading system provides precise measurement and control at low and high pressures. Resistivity measurements will provide gainful insight into the absorption process in thin films. Hopefully, modifications to the films substrate and surfaces should lower the activation energy needed for absorption. Beta flux models using MC-SET compare well with published data and should offer insights into other potential hydrogen absorbing substrates.

ACKNOWLEDGMENTS

Author Thomas Adams would like to thank Naval Surface Warfare Center, Crane Division (Crane, IN) for the Ph.D. fellowship and support in this research. This work was done while at Purdue University (West Lafayette, IN) under the direction of my advisor, with the support of my colleagues from Purdue, City Labs, Inc. (Homestead, FL) and Greenway Energy (Aiken, SC).

REFERENCES

1. Olsen, L.C., P. Cabauy, and B.J. Elkind, *Betavoltaic power sources*. Physics Today, 2012. **65**(12): p. 35-38.
2. Flanagan, T. and W. Oates, *The palladium-hydrogen system*. Annual Review of Materials Science, 1991. **21**(1): p. 269-304.
3. Lewis, F.A., *Hydrogen in palladium and palladium alloys*. International Journal of Hydrogen Energy, 1996. **21**(6): p. 461-464.
4. Adams, T.E., *Email correspondence to Joshua Schrier titled "Question on beta-voltaic device tritium storage materials"*, 2013: email on 1/10/2013.
5. Napchan, E., *MC-SET - Monte Carlo Simulation of Electron Trajectories*, 2008, [Computer Software].
6. Jenkins, J.H., et al., *Additional experimental evidence for a solar influence on nuclear decay rates*. Astroparticle Physics, 2012.
7. Rappaport, P., *The electron-voltaic effect in pn junctions induced by beta-particle bombardment*. Physical Review, 1954. **93**(1): p. 246.
8. Flicker, H., J.J. Loferski, and T.S. Elleman, *Construction of a promethium-147 atomic battery*. IEEE Transactions on Electron Devices, 1964. **11**(1): p. 2-8.
9. Manasse, F.K., J.J. Pinajian, and A.N. Tse, *Schottky barrier betavoltaic battery*. IEEE Trans. Nucl. Sci., 1976. **23**(1).
10. Olsen, L.C. *Review of betavoltaic energy conversion*. in *12th Space Photovoltaic Research and Technology Conference (SPRAT 12)*. 1993. NASA Lewis Research Center.
11. Franco, R. and M.L. Smith. *Benefits and Risks of Promethium Battery-Powered Pacemakers*. in *Advances in Pacemaker Technology*. 1974. Erlagen Springer-Verlag.
12. Kostas, T., et al., *Tritiated amorphous silicon betavoltaic devices*. IEE Proceedings-Circuits, Devices and Systems, 2003. **150**(4): p. 274-81.
13. Eiting, C.J., et al., *Demonstration of a radiation resistant, high efficiency SiC betavoltaic*. Applied Physics Letters, 2006. **88**: p. 064101.
14. Chandrashekar, M.V.S., et al., *Demonstration of a 4H SiC betavoltaic cell*. Applied Physics Letters, 2006. **88**: p. 033506.
15. DARPA, *Micro Isotope Power Sources*. BAA 06-25 Proposer Information, 2007.
16. Lamarsh, J.R. and A.J. Barratta, *Introduction to nuclear engineering*, 2001, Prentice Hall: Upper Saddle River, New Jersey.
17. Neamen, D.A., *Semiconductor physics and devices: basic principles*2003: Irwin, Inc.
18. Yoder, M.N., *Wide bandgap semiconductor materials and devices*. IEEE Transactions on Electron Devices, 1996. **43**(10): p. 1633-1636.
19. Santos, I., et al. *Molecular dynamics study of damage generation mechanisms in silicon at the low energy regime*. 2007.
20. Bower, K.E., *Polymers, phosphors, and voltaics for radioisotope microbatteries*2002: CRC.
21. Zhao, F., et al., *Buckle delamination of textured TiO₂ thin films on mica*. Thin solid films, 2005. **489**(1): p. 221-228.
22. Fishbane, P.M., S. Gasiorowicz, and S.T. Thornton, *Physics for scientists and engineers*. Vol. 2. 1996: Prentice Hall Upper Saddle River, NJ.
23. Lee, E., et al., *Hysteresis behavior of electrical resistance in Pd thin films during the process of absorption and desorption of hydrogen gas*. International Journal of Hydrogen Energy, 2010. **35**(13): p. 6984-6991.
24. Wagner, S. and A. Pundt, *Electrical resistivity and hydrogen solubility of PdH_x thin films*. Acta Materialia, 2010. **58**(4): p. 1387-1394.
25. Adams, T.E., *A Study of Palladium Thin-Films for Radioisotope Storage in Betavoltaic Power Source Designs*, in *Nuclear Engineering*2011, Purdue University: West Lafayette. p. 91.